ELSEVIER

Polymer 42 (2001) 7675–7683

polymer

www.elsevier.nl/locate/polymer

Curing and thermal ageing of elastomers as studied by ^{1}H broadband and ^{13}C high-resolution solid-state NMR

P. Palmas[a,*], L. Le Campion[a], C. Bourgeoisat[a], L. Martel[b]

[a]*Commissariat à l'Energie Atomique (CEA), Le Ripault, BP 16, 37260 Monts, France*
[b]*58 Rue Gabriel Mouilleron, 54000 Nancy, France*

Received 21 September 2000; received in revised form 13 March 2001; accepted 26 March 2001

Abstract

Curing and thermal ageing of EPDM synthetic elastomers has been studied using both ^{13}C high-resolution and ^{1}H wideline solid-state NMR experiments based on structural and dynamic parameter measurements. It is shown that cross-linking, scission and oxidation reactions can be clearly identified and quantified at concentrations as low as a few tenths percent of the carbon content. The feasibility and efficiency of two-dimensional WISE experiment for studying ageing of heterogeneous polymer-based systems has been demonstrated providing unique chemical specific dynamic information. © 2001 Elsevier Science Ltd. All rights reserved.

Keywords: Elastomer; Thermal ageing; Solid-state NMR

---

1. Introduction

A crucial component in lifetime prediction of organic materials is molecular understanding of chemical processes and kinetics involved in the course of ageing phenomenon. In polymer-based materials, chain scissions, cross-linking reactions and formation of oxidation products generally occur. As those processes are related to substantial modifications of the macromolecular backbone, strong damage in mechanical properties are expected, even at a low rate of conversion (less than 0.1%).

Highly sensitive methods such as infrared (IR) spectroscopy are generally used to elucidate molecular mechanisms and investigate specific chemical changes. Mass spectroscopy may also be applied especially for gas product analysis. Nuclear magnetic resonance (NMR) spectroscopy, and particularly solid-state NMR has been rarely employed in the field of ageing studies. This method, which is basically less sensitive presents some advantages. Firstly, it is a non-destructive bulk analysis technique as opposed to IR spectroscopy, which only probes the surface (a few micrometers) of the sample. Secondly, it provides with the same equipment both structural (in the range 10^{-10}–10^{-7} m) and dynamic (in the range 10^3–10^8 Hz) information, the latter being both, global or very local (chemical, structural or microstructural specific). Thirdly, the measurements do not suffer from data dispersion due to sample preparation or macroscopic inhomogeneities. Finally, although detection of chemical events at low concentration is usually difficult to observe directly with this technique, NMR spectroscopy is very sensitive to induced changes in molecular motions to which polymer mechanical properties are strongly correlated.

During the past 20 years, a few studies concerning the application of solid-state NMR spectroscopy to investigate ageing of elastomer network have been reported particularly concerning EPDM materials [1,2]. Structural analysis have been performed using high-resolution solid-state NMR spectra to investigate ageing processes [1–12]. Dynamic analysis studies based on relaxation time measurements have been reported principally for natural rubber and some other synthetic elastomers [11–18]. Solid-state NMR ageing investigations have also been carried out on polyethylene [19,20] and polymer blends [21]. More recently, there has been a growing interest in elastomers microimaging, which provides spatially resolved dynamic information as relaxation time contrasted images [11,14,18,22–33].

The aim of this paper is to investigate thermal ageing of ethylene, propylene, diene monomer (EPDM) elastomers using both structural and dynamic solid-state NMR techniques. Complementary methods including quantitative ^{13}C high-resolution NMR, ^{1}H broadband T_2 relaxation time,

---

[*] Corresponding author. Fax: +33-02-47-34-51-48.
E-mail address: palmas@ripault.cea.fr (P. Palmas).

0032-3861/01/$ - see front matter © 2001 Elsevier Science Ltd. All rights reserved.
PII: S0032-3861(01)00249-X

^{1}H $T_{1\rho}$ relaxation time in the rotating frame, and ^{1}H residual dipolar coupling measurements using two-dimensional wideline separation experiment (2D WISE) [34,35] have been used to investigate cross-linking, scission, oxidation processes at low rate of conversion and morphological changes. The 2D WISE technique was recently used to monitor cross-linking reactions in both crystalline phase and amorphous phase of semicrystalline polyethylene [19]. At the same time, by defining new experimental settings, Tekely et al. [36,37] demonstrated its efficiency for local field measurements on unfilled and filled natural rubber networks. In the present work, this experiment is proposed to provide valuable information on ageing study of elastomers. Solid-state NMR data obtained for non-cross-linked and cross-linked samples are first compared in order to evaluate the effects of curing. The results concerning the investigation of thermal ageing for two cross-linked polymers are then presented.

2. Experimental

2.1. Sample preparation

In this work, three different samples were analysed. Firstly, an uncross-linked elastomer mixed with 3 phr (parts per hundred rubber) of dicumyl peroxide cross-linking agent was studied. This sample is denoted as sample A. Secondly, sample A was cured under uniaxial pressure $P = 3.2 \times 10^5$ Pa at temperature $T = 180°\mathrm{C}$ to prepare a cross-linked elastomer (denoted as sample B). Finally, sample C consists of a cross-linked sample containing 1 phr of Vulcanox antioxidant. The synthetic elastomer is an ethylene propylene 1,4-hexadiene monomer (EPDM) copolymer with theoretical mass ratios $z = 72$, 22 and 6%, respectively. The elastomer, the curing agent and the anti-oxidant were obtained from commercial sources.

Samples B and C were cut into 1 mm thick pieces and thermally aged in an oven at different temperatures under atmospheric pressure or vacuum. Sample B was aged under vacuum at 200, 270°C and under atmospheric pressure at 120, 60, 70 and 80°C. Sample C was aged only under atmospheric pressure at 120°C. For each sample, sufficient amount of material were prepared to allow at least 15 different NMR experiments to be carried out. The required amount of material was removed at each ageing time for analysis.

2.2. Methods

All experiments were carried out at room temperature on a Bruker MSL300 spectrometer using standard broadband X-H CP/MAS probe (7 mm external diameter rotors) and ^{1}H selective solenoid probe (5 mm diameter tubes) for ^{1}H wideline measurements.

^{13}C high-resolution solid-state NMR spectra were recorded from a single pulse experiment using standard magic angle sample spinning (MAS) technique with spinning frequency in the range 4.5–5 kHz and high-power ^{1}H decoupling applied during acquisition. A short pulse (2 μs corresponding to flip angle $\alpha = 45°$) and a recycle time up to 5 s (which is much larger than amorphous polymer ^{13}C relaxation times) were used for quantitative analysis. High level signal/noise ratio was achieved at the expense of long experiment time requiring a high number of scans. Practically, instead of running a single long experiment, several acquisitions of smaller duration were run and free induction decays numerically added. This procedure avoids saturation of the converter's memory and provides a control of experimental stability.

^{1}H T_2 relaxation of the whole polymer system was measured using both single pulse and Hahn echo sequences.

The ^{1}H relaxation times in the rotating frame ($T_{1\rho}$) were measured using standard procedure based on a variable spin lock period preceding a constant cross-polarisation time ($T_{\mathrm{CP}} = 1$ ms) with MAS frequency $\nu_{\mathrm{r}} = 4000$ Hz. Such experimental settings allow only the highly mobile region of the polymer network to be sampled.

Proton heteronuclear dipolar spectra arising from residual dipolar local fields due to the ^{13}C-bonded protons were measured using 2D WISE experiment. Details about this technique and its applications to polymers can be found elsewhere [34,35]. In these previous works, it has been shown that heteronuclear dipolar local field information may be obtained by selecting particular experimental settings connected to the actual residual interactions of the system. The MAS-modulated ^{1}H dipolar spectra obtained appear as cross-sections in the ^{1}H dimension of the 2D experiment separated in the second dimension by the chemical shift of the ^{13}C to which the different protons are bonded. Validated first on rigid crystalline and amorphous polymers [34,35], this approach has been recently used for natural rubber applications [36,37].

In the present work, the synthetic EPDM elastomer sample exhibits a more rigid behaviour than natural rubber. Moreover, concentrations of ca. 10% of crystalline areas were estimated from DSC measurements. Two different experiments have been carried out to investigate the dynamics of such systems: two sets of parameters ($T_{\mathrm{CP}} = 2$ ms, $\nu_{\mathrm{r}} = 800$ Hz) and ($T_{\mathrm{CP}} = 200$ μs, $\nu_{\mathrm{r}} = 4$ kHz) were used to sample the protons located in soft and rigid domains, respectively. These experiments are referred to as 'soft WISE' and 'rigid WISE' experiments hereafter. During the evolution period of the WISE experiment, chemical shift effects can be neglected for highly rigid systems with strong dipolar interactions. However, these effects may become important for highly mobile systems like natural rubber [37]. In that case, the experiment should be repeated for each proton chemical shift put on resonance. As far as the EPDM polymer is concerned, the proton chemical shift dispersion is small compared to residual dipolar interaction. Consequently, the chemical shift effects

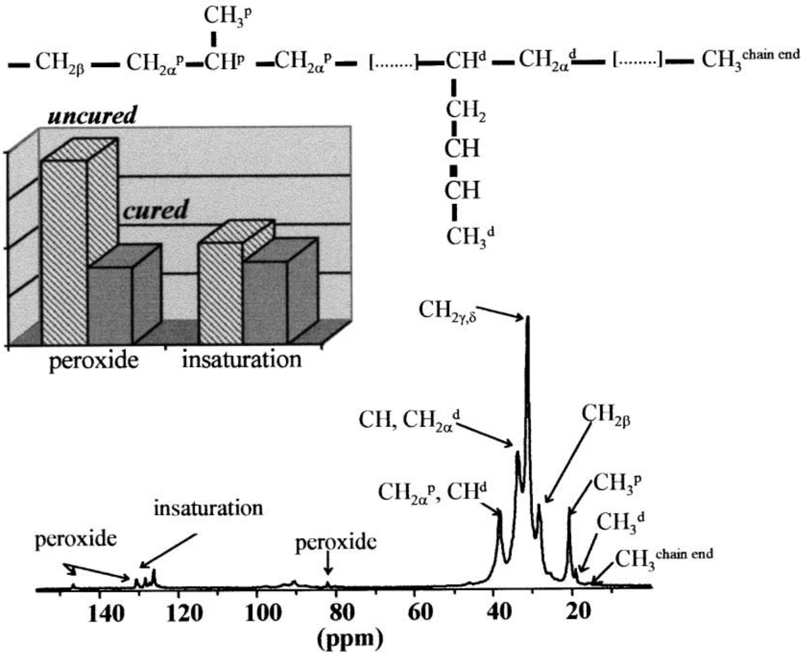

Fig. 1. (From top to bottom) EPDM molecule chemical formula; peroxide and unsaturation ratio for uncured and cured elastomer; ^{13}C high-resolution solid-state NMR spectrum of sample A (uncured sample).

are reduced by selecting the ^{1}H carrier frequency in the middle of the aliphatic region.

3. Results and discussion

3.1. Curing process

The ^{13}C high-resolution solid-state MAS NMR spectrum of sample A (uncured polymer) is shown in Fig. 1. Synthetic elastomers like natural rubber are known to provide solution-like quality spectra in the solid-state. This is due to the fact that fast local molecular motion occurs at temperatures of use that are much larger than the glass transition temperature. Thanks to the high sensitivity and resolution, a number of lines could be assigned in the basis of published results obtained in solution [38]. The spectrum can be quantitatively analysed by performing a careful line integration. As a result, the polymer composition can be evaluated leading to monomer concentrations (ethylene: 75.3%, propylene: 18.6%, hexadiene: 6.1%) and peroxide concentration (2.4%), which are in close agreement with theoretical values (72, 22, 6 and 2.9%, respectively). The intensity errors obtained from line integration essentially depend on data treatment including window function, phasing and baseline correction. The precision of measurement strongly depends on the signal/noise ratio and spectral resolution. In this work, the experimental precision was estimated using the dispersion of values derived from five data treatments of sample A. Relatives errors of 5, 5 and 10% were obtained for peroxide, diene unsaturation and methyl chain end, respectively.

Results obtained from the ^{1}H wideline measurements of samples A and B are summarised in Table 1. ^{1}H T_2 relaxation decay from Hahn echo and single pulse experiments was satisfactorily fitted assuming two components, which include exponential and gaussian decay. The exponential decay accounts for the mobile regions, i.e. those containing highly mobile polymer fragments. The gaussian decay accounts for the hard regions of the material, i.e. those containing less mobile polymer fragments. In each case, experimental data were well fitted providing the mobile phase ratio (x), the relaxation rate in the mobile phase ($1/T_{2m}$) and the pseudo-relaxation rate in the rigid

Table 1
^{1}H transversal relaxation rate in the mobile phase and rigid phase, extracted, respectively, from Hahn echo and one pulse experiments; mobile phase ratio from Hahn echo experiment; ^{1}H relaxation rate in the rotating frame of protons from different functional groups from $T_{1\rho}$ measurements. Relaxation rates are given in s^{-1}

	$1/T_{2m}$	x	$1/T_{2r}$	$1/T_{1\rho}$ (CH_{3p})	$1/T_{1\rho}$ ($CH_{2\beta}$, $CH_{\beta\beta}$)	$1/T_{1\rho}$ ($CH_2\gamma_{,\delta>}$)	$1/T_{1\rho}$ (CH^{p})	$1/T_{1\rho}$ ($CH_{2\alpha}$, CH^{d})
Uncured	4501	0.67	63,970	201	287	297	297	282
Cured	6178	0.73	50,431	229	338	346	379	366

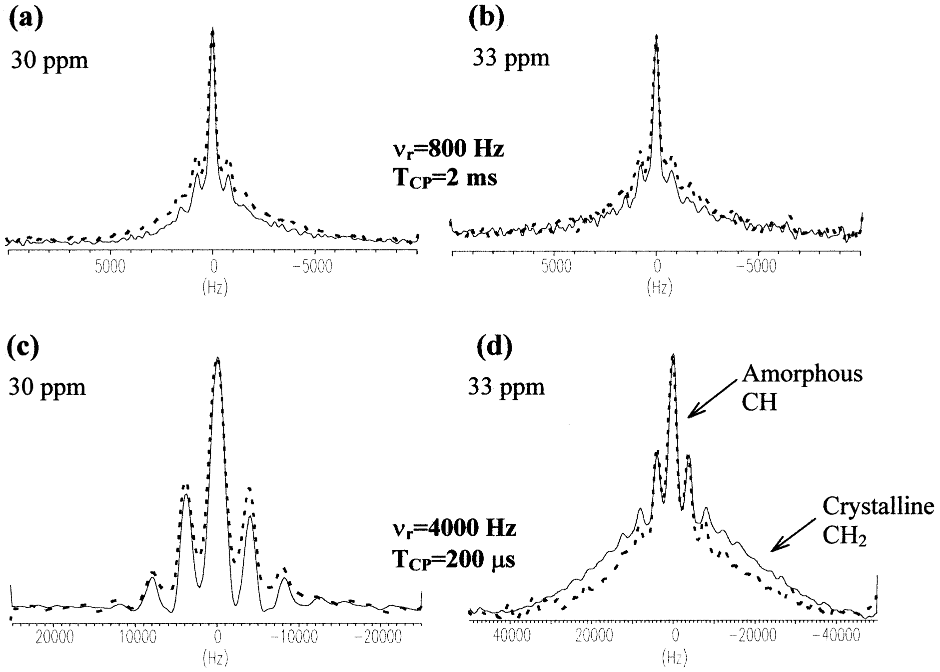

Fig. 2. MAS modulated ^{1}H dipolar spectra for soft domains (a) and (b) and rigid domains (c) and (d) extracted from 2D map for the two different ^{13}C chemical shifts $\delta = 30$ and 33 ppm. Solid and dotted lines stand, respectively, for non-cured and cured samples.

phase ($1/T_{2r}$). The latter is related to the residual part of the second moment qM_2 of the dipolar interaction as follows: $1/T_{2r} = (qM_2)^{1/2}$. The relaxation function used in the present work is a simplification of the conventional function used for rubber systems [17]. The t/T_{2m} term is neglected compared to $t^2/2T_{2r}^2$ term. Even for short times, this approximation is justified according to the relaxation times of the present system. Within this simple approach, the rigid phase is supposed to include protons belonging to the microcrystalline domains (the latter consists of polyethylene fragments) as well as protons located in the amorphous domains close to cross-links, entanglements or microcrystalline domain itself. Consequently, the mobile phase includes all other protons and particularly dangling chains.

Single pulse experiments were carried out on four different samples to evaluate the precision of the T_2 relaxation measurements. Experimental errors less than 4 and 3% were obtained for T_{2m} and T_{2r}, respectively.

The $T_{1\rho}$ values of protons attached to carbon atoms were extracted by fitting the experimental data with single exponential decay (also given in Table 1).

Dipolar slices modulated by MAS (shown in Fig. 2) were extracted from 2D map of rigid WISE and soft WISE experiments, for each of the different ^{13}C chemical shifts that were detected. In both cases, a strong modulation by MAS as revealed by well-defined spinning sidebands can be observed indicating the inhomogeneous character of the dipolar spectra. As already shown in previous works [34,35], the envelope of such a spinning sidebands is a direct visualisation of the residual dipolar interaction experienced by the different ^{13}C-bonded protons.

Spectral simulation and fit to experimental data may be carried out in order to extract quantitative information on residual dipolar heteronuclear interactions. Such spectral analyses were performed for C–H moieties [35] in more or less rigid polymers. For cross-linked natural rubber, two components with different dipolar couplings were considered [36,37]. However, as mentioned previously, this two-component approach is a first approximation and is consistent with a distribution of correlation times in polymer chains. Although useful, such a simulation is not essential in the scope of the present study aimed at emphasising the availability to detect changes during curing and ageing of synthetic elastomer-based heterogeneous materials.

As far as the curing effects are concerned, the following observations can be made from the examination of the whole set of NMR results. Firstly, there is a net decrease in the signal intensity of peroxide and diene unsaturation. Secondly, a large increase in the relaxation rate in the mobile phase ($1/T_{2m}$) is observed using single pulse and Hahn echo experiments (15 and 37%, respectively). A small decrease in the relaxation rate in rigid domains ($1/T_{2r}$) and a small increase in the mobile phase ratio are also shown. Thirdly, an increase in relaxation rates in the rotating frame ($T_{1\rho}$) of each proton is observed. This effect is more pronounced for CH and $CH_{2\alpha}$ groups, which are expected to be located close to joints like sidechains or cross-links. Finally, an increase in the first sidebands relative intensity is also evidenced in dipolar slices extracted

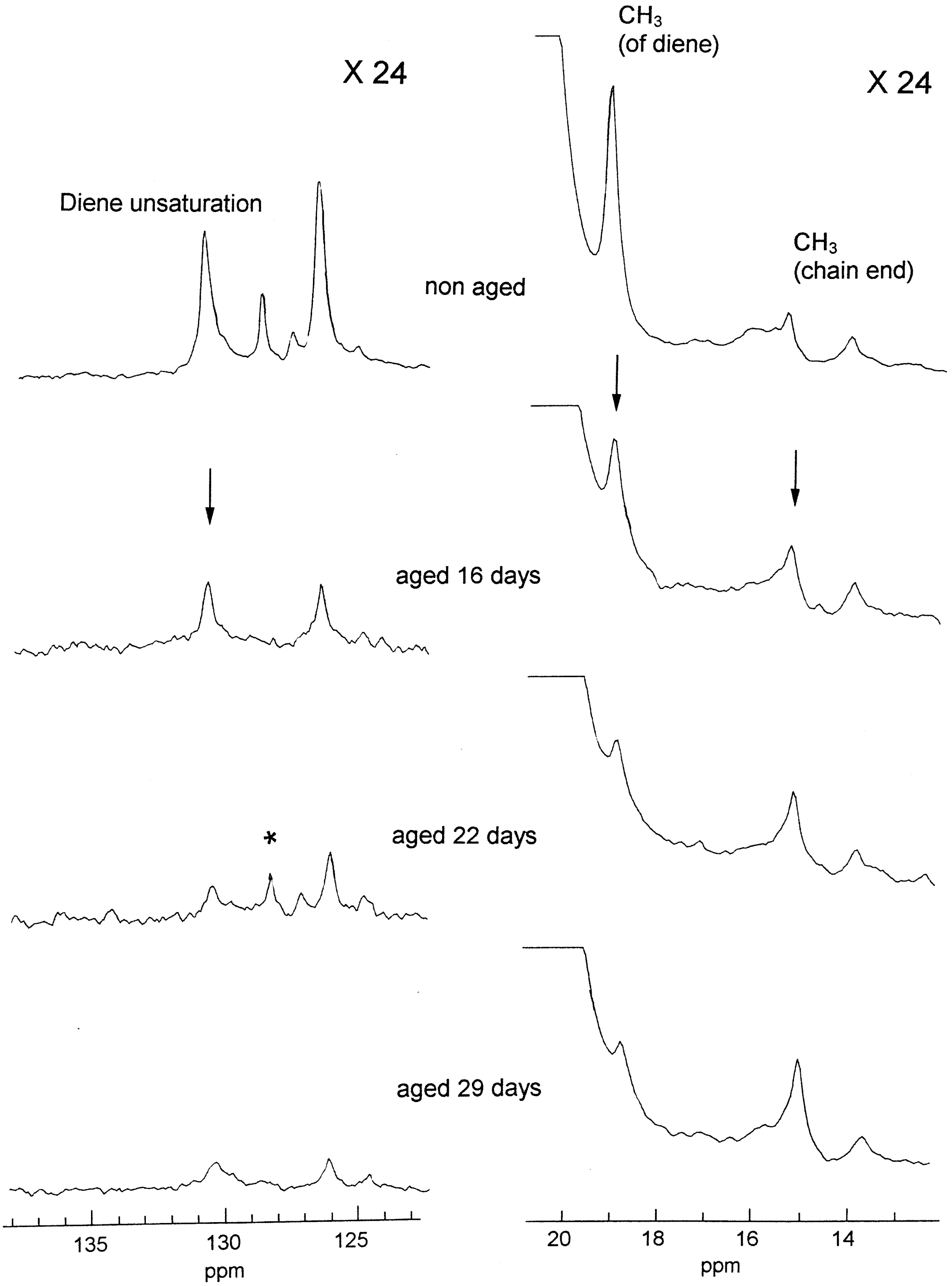

Fig. 3. Anaerobic ageing 13 days at 200°C followed by 16 days at 270°C. ^{13}C high-resolution solid-state NMR spectrum as a function of ageing time, expansion of regions of aliphatic and unsaturated carbons. The asterisk indicates an extra peak due to data treatment artefact, which has not to be taken into account. Arrows indicate signal belonging to diene unsaturation, methyl of diene and methyl chain end in which intensity change as a function of ageing time.

from 2D soft WISE (Fig. 2a and b) and rigid WISE (Fig. 2c) experiments. It is obvious from Fig. 2 that the residual dipolar coupling experienced by protons belonging to amorphous polymer regions is increased by the vulcanisation process.

Examination of the dipolar slice at ^{13}C chemical shift $\delta = 33$ ppm from rigid WISE experiment (see Fig. 2d) provides another specific information. Actually, the dipolar spectrum consists of the superposition of two components with the same ^{13}C chemical shift: (i) an inhomogeneously broadened MAS modulated spectrum due to CH in the amorphous domain and roughly identical to spectrum 3 c; (ii) an homogeneously broadened large dipolar spectrum due to CH_2 moieties in the crystalline domains. It is clear

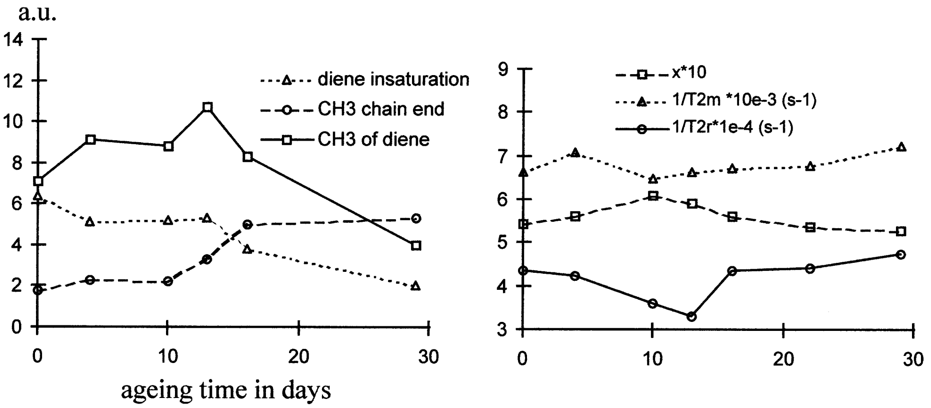

Fig. 4. Anaerobic ageing 13 days at 200°C followed by 16 days at 270°C: (left) the course of diene unsaturation, methyl chain end and methyl of diene during EPDM elastomer ageing, as measured from ^{13}C high-resolution solid-state NMR spectra; (right) the course of mobile phase ratio (x), relaxation rate in the mobile phase ($1/T_{2m}$) and rigid phase ($1/T_{2r}$) as a function of ageing time, extracted from one pulse experiment.

from Fig. 2 that a decrease in the crystalline ratio is induced by the curing process while a global hardening of the amorphous region is observed. This important result has to be related to the unexpected apparent decrease in the rigid relaxation rate $1/T_{2r}$ and to the increase in the mobile phase ratio (x) from T_2 measurements. Using only these results, any interpretation exclusively based on mobility considerations would lead to erroneous conclusions. Only spatially and chemical shift-resolved information provided by 2D NMR spectroscopy can give a precise description of transformations occurring in such heterogeneous materials.

The experimentally observed decrease of crystallinity may be explained by a loss of mobility of polymer chains due to cross-linking. In fact, microcrystalline domains mainly result from polyethylene fragments $(CH_2)_n$, which can gather and acquire crystalline order. This process is expected to be more or less hampered by cross-linking, which reduces the number of degrees of freedom and the mobility of macromolecular chains.

As a conclusion, the combination of high- and low-resolution NMR techniques has experimentally shown that curing process of samples containing dicumyl peroxide induces a substantial hardening of the whole amorphous part of the polymer. This is due to cross-linking reactions involving dangling diene unsaturations. A decrease in crystallinity is observed during this process.

3.2. Ageing at high temperatures

Sample B was aged under vacuum for a period of 13 days at 200°C followed by 16 days at 270°C. ^{13}C high-resolution spectra and ^{1}H T_2 wideline measurements carried out at several ageing times during the total period of 29 days, are shown in Figs. 3 and 4. Evidence of chain scission at the beginning of the ageing period is revealed by a gradual increase of methyl end chain signal intensity in the high-resolution solid-state NMR spectra. This is confirmed by the increase of the mobile phase ratio (x) and the decrease of the relaxation rate in the rigid phase ($1/T_{2r}$), consistent with an initial increase of mobility of the system. At 270°C, chain scissions still occur. At the same time, a fast decrease of diene unsaturation ratio together with the net increase of both relaxation rates can be observed indicating that cross-linking reactions take place and become the main process.

Like anaerobic ageing, aerobic ageing of the same sample exhibits a fast decrease of unsaturation ratio together with a rapid increase of methyl chain end intensity for a short

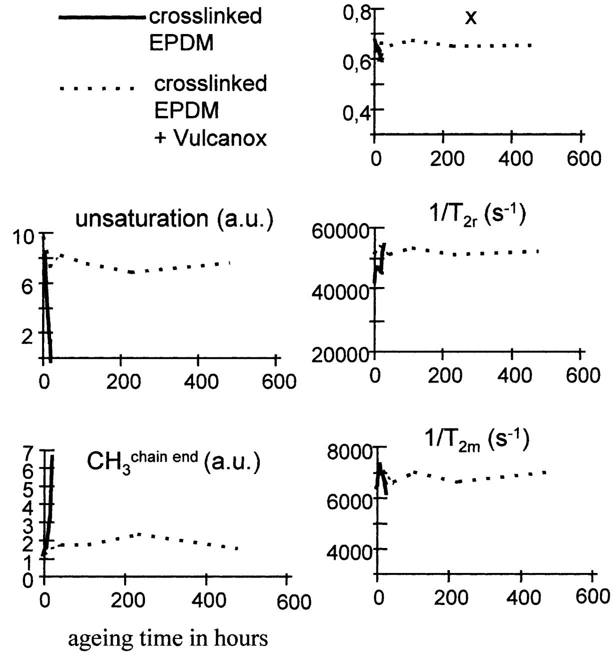

Fig. 5. Aerobic ageing at 120°C. The course of diene unsaturation and methyl chain end (on the left) and mobile phase ratio (x), relaxation rate in the mobile phase ($1/T_{2m}$) and rigid phase ($1/T_{2r}$) (on the right) as a function of ageing time; values extracted from ^{13}C high-resolution solid-state NMR spectra and ^{1}H wideline (one pulse experiment) measurements.

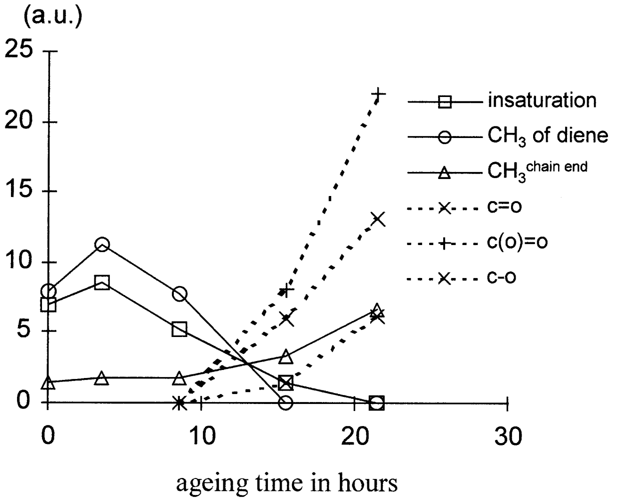

Fig. 6. Aerobic ageing at 120°C. The course of diene unsaturation, methyl chain end, methyl from diene (solid lines) and oxidation products like ketones, ester or acid, alcohol or ether (dotted lines) as a function of ageing time.

period of 22 h at a lower ageing temperature T (120°C) (Figs. 5 and 6). These results indicate a very high activation of scission and cross-linking reactions by the presence of high oxygen concentration when compared with anaerobic ageing. These reactions occur before the appearance of oxidation products (alcohol, ketone, ester, acid) that were detected only after 10 h. Changes in molecular motion sensitive parameters can also be noted. Firstly, an increase of the rigid phase relaxation rate ($1/T_{2r}$) is observed. Secondly, an initial increase followed by a decrease of the mobile phase relaxation rate ($1/T_{2m}$) is seen. Finally, a gradual decrease of the mobile phase ratio (x) is shown. Whereas strong modifications of the NMR parameters are observed for pure polymer, results obtained for sample C (the compound containing the antioxidant Vulcanox) indicate an extreme stability toward thermal ageing for a period of 22 days. In that case, except small oscillations, there were no significant changes of NMR parameters such as line intensities and relaxation times and no oxidation product was detected.

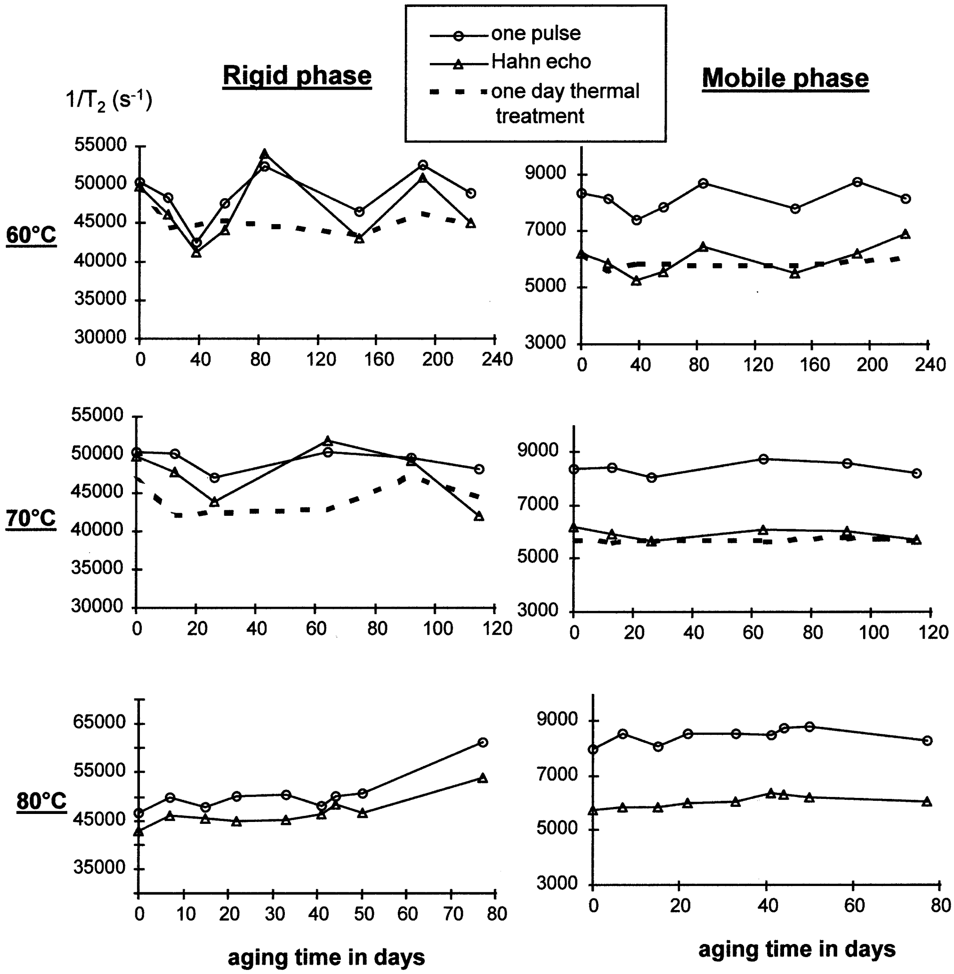

Fig. 7. Aerobic ageing at 60, 70 and 80°C. The course of relaxation rate in the rigid and mobile phase as a function of ageing time. Values obtained from one pulse and Hahn echo experiments. The dotted line corresponds to results obtained from Hahn echo measurements performed after an additional 1-day thermal treatment.

Table 2
Ageing rate in the rigid phase (left) extracted from one pulse measurements and ageing rate in the mobile phase (right) extracted from Hahn echo experiment at three different ageing temperatures

Ageing temperatures (°C)	$d(1/T_{2r})/dt$ (s^{-2})	$d(1/T_{2m})/dt$ (s^{-2})
60	13	1.9
70	26	2.9
80	140	6.0

3.3. Ageing at low temperatures

After careful examination of highly sensitive ^{13}C high-resolution NMR spectra of samples B thermally aged at different temperatures, ($T = 60$, 70 and 80°C) no changes in line intensities can be observed indicating that no oxidation products nor chemical group concentration variations are detected in the bulk sample. In spite of that, significant evolution could be observed in NMR relaxation parameters for the different ageing conditions. Graph of $1/T_2$ as a function of ageing time is shown in Fig. 7.

Globally, and to a first approximation, an increase of both relaxation rates $1/T_{2m}$ and $1/T_{2r}$ can be noted. Mobile phase ratio (x) is roughly constant. This is consistent with the gradual hardening of the network. The second stage decrease in $1/T_{2m}$ observed for longer ageing times at $T = 120$°C is not observed in that case. Fits according to a simple linear equation were performed to give an evaluation of the rate of the hardening process. To get rid of the oscillations observed for ageing at 60 and 70°C, the calculations were carried out on the data recorded after a single day thermal treatment (Fig. 7) (vide supra). Within experimental errors, a gradual increase of the ageing rate $d(1/T_2)/dt$ (s^{-1}/day) as a function of ageing temperature is observed (see Table 2).

In addition to the global increase in the relaxation rate, strong oscillations are observed in both T_{2r} and T_{2m} relaxation parameters as a function of ageing time. This effect, which is strong for ageing at 60 and 70°C with respective quantitative periods $T \approx 50$ and 40 days, was not observed at 80°C. These oscillations were also evidenced from $T_{1\rho}$ measurements and from 2D rigid and soft WISE experiments by tracing dipolar sideband (centre-band intensity constant) as a function of ageing time (Fig.8), showing the sensitivity of this experiment. Moreover, a global decrease in the ratio is evidenced in that case. A possible explanation of this observed increase in the contribution of the central line may be the H–H spin diffusion efficiency growing effect due to higher proton–proton residual dipolar interaction or higher incoherent relaxation effect as revealed by T_2 Hahn echo measurements [37]. However, it should be noted that the data might be altered by possible experimental instability or RF performance during the long period of ageing time. Such instability is inherent to class C amplifier and is expected to induce significant effects on the cross polarisation transfer process. However, such unwanted effect should be overcome by using existing class A amplifier.

The oscillations observed in the graph of $1/T_2$ vs. ageing time are probably due to reversible phenomena occurring in

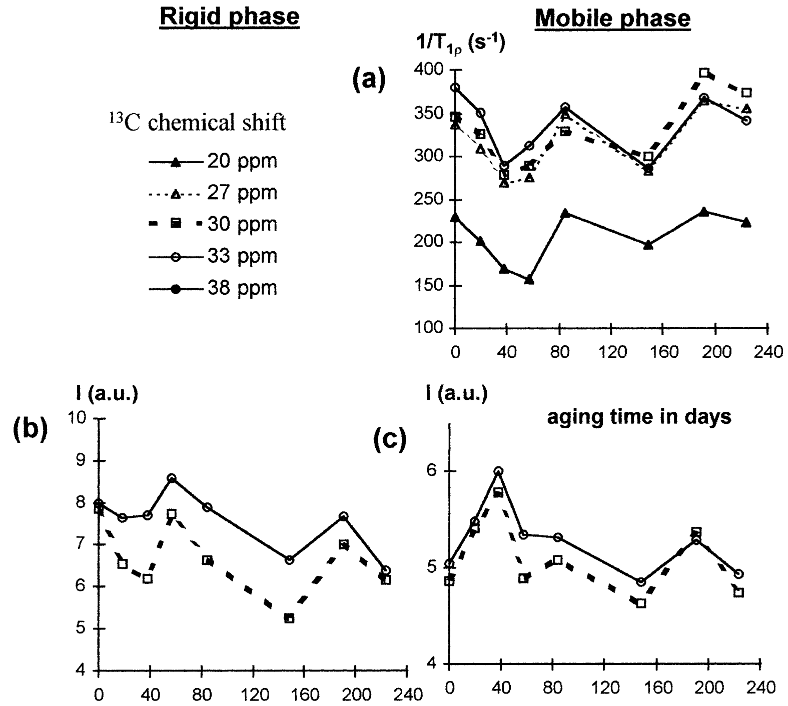

Fig. 8. Aerobic ageing at 60°C. The course of relaxation rate in the ^{1}H rotating frame (a) and first sidebands intensity (in arbitrary unit, centre band kept as constant) of dipolar spectra extracted from rigid WISE (b) and soft WISE (c) experiments as a function of ageing time.

the amorphous or in the intermediate interfacial region during ageing. They are consistent with changing physical constraints as a function of ageing time. Actually, viscoelastic phenomena are expected to dominate physicochemical mechanisms at low temperature. Three remarks support this assumption. Firstly, as a result of superposing dipolar slices at ^{13}C chemical shift $\delta = 33$ ppm (not shown), no variation of crystalline ratio happened during ageing providing that the observed oscillations exclusively occur in the amorphous or in the interfacial regions. Secondly, no changes were detected on ^{13}C high-resolution NMR spectra. Finally, the oscillations disappeared when performing new measurements after an additional 1-day thermal treatment (as shown in Fig. 7).

4. Conclusion

It has been shown that solid-state NMR is sensitive to thermal ageing occurring in elastomers. Using a combination of highly sensitive high-resolution spectra, relaxation time measurements and 2D WISE experiments, chemical reactions like cross-linking, scission and oxidation can be identified at concentrations as low as a few tenths of percent of the carbon content. Concerning 2D experiment, its efficiency to investigate curing and thermal ageing has been demonstrated. All these methods are now being applied for ageing studies performed under γ-radiation at low doses.

It is important to note that long period of time inherent to slowly accelerated ageing conditions require a great stability of spectrometer settings, which are difficult to guarantee with class C amplifier. Such stability of pulse amplitude and shape can be obtained using class A amplifier generation. Within such conditions of stability, 2D experiments, which provide chemical shift specific dynamic information are expected to be very interesting for ageing studies of heterogeneous polymer-based systems like copolymers, polymer blends and composites.

Acknowledgements

This work is part of the COMOR (Comportement des Matériaux Organiques sous Rayonnement) organisation activities inside CEA. We are very grateful to Dr Stéphanie Labayle Camus for improvements of the manuscript.

References

[1] O'Donnell JH, Whittaker AK. Polymer 1992;33(1):62–7.
[2] O'Donnell JH, Whittaker AK. Br Polym J 1985;17(1):51–5.
[3] Parker DD, Koenig JL. Polym Mater Sci Engng 1997;76:193.
[4] Parker DD, Koenig JL. J Appl Polym Sci 1998;70(7):1371–83.
[5] Li S, He L. Xiangjiao Gongye 1993;40(2):111–8.
[6] Wu Z, Yang W. Xiangjiao Gongye 1994;41(4):217–29.
[7] Kinsey RA. Rubber Chem Technol 1990;63(3):407–25.
[8] Patterson DJ, Shields CM, Cholli A, Koenig JL. Polym Prepr (Am Chem Soc, Div Polym Chem) 1984;25(1):358–9.
[9] Guerry JL. Rev Gen Caoutch Plast 1977;54(575):103–7.
[10] Barron PF, O'Donnell JH, Whittaker AK. Polym Bull 1985;14:339–46.
[11] Fuelber C, Bluemich B, Unseld K, Herrmann V. Kautsch Gummi Kunstst 1995;48(4):254–9.
[12] Zhang P, Lan H, Tang X. Gaofenzi Cailiao Kezue Yu Gongcheng 1989;5(6):55–60.
[13] Kahle M, Götz H, Palm K. Int Wiss Kolloq, Tech Hochsch Ilmenau 1974;19(1):9–15.
[14] Knoergen M, Heuert U, Menge H, Schneider H. Angew Makromol Chem 1998;261/263(4623):123–33.
[15] Denner P, Walter B, Willing T. Macromol Symp 1997;119:339–52.
[16] Smith TB, Roy AK, Tanzer CI. PCT Int Appl Patent No. WO 97/42516, p. 57.
[17] Pentimalli M, Capitani D, Ferrando A, Ferri D, Ragni P, Segre AL. Polymer 2000;41:2871–81.
[18] Knörgen M, Heuert U, Schneider H, Barth P, Kuhn W. Polym Bull 1997;38:101–8.
[19] Beckham HW, Spiess HW. Macromol Chem Phys 1994;195(5):1471–82.
[20] Okazaki M, Nunome K, Toriyama K. Nagoya Kogyo Gijutsu Shikensho Hokoku 1990;39(9/10):379–87.
[21] Wastlund C, Schmidt M, Schantz S, Maurer FHJ. Polym Engng Sci 1998;38(8):1286–94.
[22] Kuhn W, Barth P, Denner P, Mueller R. Solid State Nucl Magn Reson 1996;6(4):295–308.
[23] Hafner S, Barth P. Magn Reson Imaging 1995;13(5):739–44.
[24] Barth P, Hafner S. Magn Reson Imaging 1997;15(1):107–12.
[25] Kuhn W, Theis I, Koeller E. Mater Res Soc Symp Proc (Adv Tomogr Imaging Meth Anal Mater) 1991;217:33–42.
[26] Kuhn W, Koeller E, Theis I. In: Bluemich B, Kuhn W, editors. Magn reson microsc, Weinheim, Germany: VCH, 1992. p. 217–35.
[27] Mark JE. Chemtracts: Macromol Chem 1992;3(1):24–7.
[28] Krejsa MR, Koenig JL. Rubber Chem Technol 1991;64(4):635–40.
[29] Bluemler P, Bluemich B. Macromolecules 1991;24(9):2183–8.
[30] Bluemler P, Bluemich B, Dumler H. Kautsch Gummi Kunstst 1992;45(9):699–702.
[31] Barth P, Hafner S, Kuhn W. J Magn Reson Ser A 1994;110(2):198–201.
[32] Bluemich B, Bluemler P, Guenther E, Schauss G, Spiess HW. Makromol Chem, Macromol Symp (Fourth German–USSR Symp Polym Sci, 1990) 1991;44:37–45.
[33] Oh SJ, Koenig JL. Polymer 1999;40:4703–8.
[34] Tekely P, Palmas P, Mutzenhardt P. Macromolecules 1993;26:7363.
[35] Palmas P, Tekely P, Canet D. Solid State Nucl Magn Reson 1995;4:105.
[36] Malveau C, Tekely P, Canet D. Solid State Nucl Magn Reson 1997;7:271–80.
[37] Eulry V, Tekely P, Humbert F, Canet D, Marcilloux J. Polymer 2000;41:3405.
[38] Pooter MD, Smith PB, Dohrer KK, Bennett KF, Meadows MD, Smith CG, Schouwenaars HP, Geerards RA. J Appl Polym Sci 1991;42:399.